Inactivation of a protein hydroxylase complex impairs replication fork restart in cancer and neurodevelopmental disorders

Tristan J Kennedy[1#], Sally C Fletcher[1#], Uncaar Boora[1], Erin Fraser-Williams[1], Arashpreet Kaur[1], Gareth W Hughes[1], Eline Hendrix[1], Joanna R Morris[1], Stephen J Smerdon[1], and Mathew L Coleman[1,2]

[1]Department of Cancer and Genomic Sciences, University of Birmingham, Birmingham, B15 2TT, UK
[2]To whom correspondence should be addressed: m.coleman@bham.ac.uk
[#]contributed equally

Abstract

Protein hydroxylation is a post-translational modification that is commonly catalysed by enzymes of the oxygen- and 2-oxoglutarate (2OG)-dependent oxygenase family. The Jumonji-C (JmjC)-only sub-family of 2OG-oxygenases catalyse the hydroxylation of protein and tRNA substrates involved in fundamental cellular processes. Jumonji-domain 5 (JMJD5) is a highly conserved and essential 2OG-oxygenase that, thus far, is the only arginyl hydroxylase assigned in eukaryotes. We recently reported that JMJD5 hydroxylase activity is required for DNA replication fidelity, and that pathogenic variants cause replication stress (RS) and genome instability (GIN) in a novel neurodevelopmental disorder. Because of the prevalence of RS and GIN in cancer, and reported roles of JMJD5 in tumorigenesis, we here investigate the impact of JMJD5 cancer mutations on its role in replication fidelity. We describe the structural impact of cancer missense mutations on the hydroxylase activity of JMJD5 and its interaction with 'RCCD1', an abundant binding partner encoded by a gene associated with susceptibility to a variety of tumour types. We show that the JMJD5:RCCD1 interaction is disrupted by cancer mutations and that the complex is essential for suppressing RS and GIN in tumour cells. Finally, we describe a novel interaction of the complex with RAD51 paralogues and demonstrate the importance of the JMJD5:RCCD1 interaction for normal replication fork restart. Our findings further highlight the importance of protein hydroxylases in fundamental cellular processes and the consequences of JMJD5 and RCCD1 deregulation in human disease.

Keywords: JMJD5, RCCD1, replication stress, genome instability, cancer, neurodevelopmental disorder, DNA damage, protein hydroxylase

36 **Introduction**

37 Mechanistic insight into the basis of disease often follows the characterisation of novel post-
38 translational modifications (PTMs). First reported as a fibrillar collagen modification, protein
39 hydroxylation is the enzymatic incorporation of a single oxygen atom into an amino acid
40 sidechain [1, 2]. Although, the essential role of protein hydroxylation as an oxygen sensor in
41 response to hypoxia has linked the modification intrinsically with disease, it remains poorly
42 characterised compared to other PTMs [3].

43 The enzymatic family responsible for catalysis of most protein hydroxylation are known as
44 2OG-oxygenases. Named for their reliance on molecular oxygen, Fe(II) and the Krebs cycle
45 intermediate 2OG as co-factors, these enzymes have been shown to catalyse a range of
46 oxidative modifications on proteins, nucleic acids and lipids [4-6]. This diversity in substrate
47 targets has involved 2OG-oxygenases in many facets of cellular biology. One fundamental
48 pathway involving oxygenation is gene expression, with 2OG-oxygenases identified that
49 control transcription, splicing and translation.

50 The epigenetic modification of histone tails plays a key role in regulating gene transcription
51 and chromatin structure [7]. The lysine histone demethylases (KDMs) belong to a subfamily
52 of phylogenetically distinct 2OG-oxygenases called Jumonji-C (JmjC) enzymes, which are
53 named after their characteristic catalytic JmjC domain [8]. Epigenetic regulation by KDMs, and
54 its link to human development and disease, has been extensively characterised. However,
55 other JmjC oxygenases with links to gene expression and disease require more
56 comprehensive investigation [5, 9].

57 JmjC domain protein 5 (JMJD5) is an enigmatic 2OG-oxygenase that is essential for life [10].
58 JMJD5 belongs to the 'JmjC-only' sub-family which, although sharing similarities to KDMs in
59 their catalytic domains, catalyse stable protein hydroxylation rather than demethylation [8].
60 JMJD5 was originally reported as a KDM, but more recently has been shown to catalyse stable
61 arginyl hydroxylation *in vitro* [11, 12]. We have recently identified human JMJD5 variants that
62 are deleterious to splicing and hydroxylase stability and activity, and that cause a
63 developmental disorder associated with growth delay, intellectual disability, and facial
64 dysmorphism [13]. This clinical phenotype was associated with an increase in RS, which is
65 now recognised as major driver of GIN, including in tumour cells [14]. Although JMJD5 has
66 been linked to cancer [15-19], its importance for replication fidelity and genome stability in this
67 context is unclear. Whether JMJD5 is mutationally inactivated in tumour cells, and the role of
68 this in cancer-associated RS and GIN, is not known.

69 Here we investigate the role of JMJD5 in replication fidelity using tumour cell models. We
70 describe how JMJD5 is mutated and functionally impaired in a variety of cancers, and that

these variants fail to suppress RS. Tumour variants also prevent the interaction of JMJD5 with a novel cancer susceptibility gene product called RCCD1. By discovering interactors of this hydroxylase complex, we assign the function of JMJD5 and RCCD1 to replication fork re-start in both cancer and primary cells derived from neurodevelopmental disorder patients. Our findings provide critical new insights into protein hydroxylase biology, and a solid foundation for mechanistic and preclinical studies of the JMJD5:RCCD1 pathway.

Results

JMJD5 knockdown increases basal and stress-induced replication stress in tumour cell models

Our previous work uncovered a role for JMJD5 activity in replication fidelity using patient-derived dermal fibroblasts as a model [13]. To begin to explore the replication role of JMJD5 in other cell types and in cancer, we tested whether JMJD5 controls replication fidelity in four commonly used tumour cell lines; lung and cervical adenocarcinoma epithelial cells (A549 and HeLa, respectively) and bone osteosarcoma cells (U2OS and Saos-2). Following JMJD5 knockdown (Figure 1A and Supplemental Figure 1A/D/G), we quantified micronuclei and 53BP1 bodies as indirect markers of replication stress. Increased micronuclei (Figure 1B, upper panel) were observed in all four models following treatment with two independent JMJD5 siRNAs (Figure 1B, lower panel; Supplemental Figure 1B/E/H). Likewise, we observed increased 53BP1 bodies (Figure 1C, upper panel) following JMJD5 knockdown in each of the cancer cell lines (Figure 1C, lower panel, and Supplemental Figure 1C/F/I).

Next, we used single molecule DNA fibre analysis to quantify stalled forks (Figure 1D), which increased during replication stress and following JMJD5 loss-of-function, as reported previously in primary dermal fibroblasts [13]. Stalled forks were elevated in A549 and U2OS cells in response to JMJD5 knockdown (Figure 1E and Supplemental Figure 2A), which was further exacerbated by the ribonucleotide reductase inhibitor hydroxyurea (HU) (Supplemental Figure 2B/C).

Unperturbed DNA replication proceeds bidirectionally from the same origin with comparable speeds, resulting in replication fork ‘symmetry’. Perturbed DNA replication may result in ‘fork asymmetry’, resulting from a slowing, pausing or collapsing of one of the two replication forks. Consistent with perturbed DNA replication, we observed significantly increased fork asymmetry following JMJD5 knockdown in A549 cells, both in the absence (Figure 1F) and presence (Supplemental Figure 2D) of HU. Likewise, we observed significant increases in fork asymmetry following JMJD5 knockdown in U2OS cells, both with and without HU treatment

105 (Supplemental Figure 2E-F). Together, these results suggest that JMJD5 controls replication
106 fidelity and genome stability in a variety of cell types and cancer models.
107
108 **JMJD5 is functionally inactivated by cancer variants**
109 Tumour suppressor genes (TSGs) that control genome stability are functionally inactivated by
110 a variety of mechanisms in cancer cells. Inherited variants in such genes can also cause
111 susceptibility to cancer and early onset of the disease. Interestingly, two siblings affected by
112 the previously described neurodevelopmental disorder inherited one of their bilateral
113 inactivating JMJD5 mutations (C123Y) from their mother, who suffered from early onset breast
114 cancer [13]. Her tumour genome did not contain known driver mutations (Illumina TruSight
115 Oncology panel sequencing of 94 genes), raising the possibility that the JMJD5 missense
116 variant contributed to her disease. Whether somatic JMJD5 tumour mutations also exist, and
117 the potential role of these in RS, GIN, and tumourigenesis, is not known.
118
119 To investigate whether *JMJD5* is mutated in cancer, we mined tumour sequencing databases
120 (Supplementary Table 1) and plotted variants against the JMJD5 protein sequence (Figure
121 2A). Missense substitutions, truncations and in-frame deletions were observed throughout the
122 enzyme and in all three structural motifs including the N-terminal domain, JmjC extension and
123 JmjC catalytic domain. Consistent with potential functional consequences, mutations were
124 also recurrent and clustered in hotspots (Figure 2A). To investigate the impact of tumour-
125 associated mutations on JMJD5 function, we cloned a panel of 28 cancer mutants, focussing
126 on variants affecting conserved residues in key structural regions and with predicted functional
127 impact (Supplementary Table 1, 2, Supplemental Figure 3). To investigate whether any of
128 these variants compromised JMJD5 protein expression, we transfected HeLa cells with HA-
129 tagged JMJD5 cancer mutants. Western blot analysis indicated that 12/28 variants negatively
130 affected JMJD5 expression with six variants having a severe impact on protein expression.
131 (Figure 2B, Supplementary Table 2). Next, we tested whether any of the variants negatively
132 impacted JMJD5 catalytic activity using recombinant JMJD5 cancer mutants and an *in vitro*
133 hydroxylation assay (as previously described [13]). Half of the cancer mutants displayed
134 significantly reduced hydroxylase activity in comparison to WT JMJD5 (Figure 2C)
135 (Supplementary Table 2). Overall, these data indicate that cancer mutants negatively impact
136 JMJD5 expression and hydroxylase activity. Whether the apparently benign mutants
137 (Supplementary Table 1) negatively affect function, but through alternative mechanisms,
138 remains unclear.
139
140 **JMJD5 cancer variants are unable to restore normal replication fidelity**

141 Our previous work demonstrated that a disease-associated missense variant (C123Y)
142 impaired JMJD5 hydroxylase activity, and that the role of JMJD5 in replication fidelity is
143 activity-dependent [13]. Therefore, we hypothesized that cancer-associated missense variants
144 that impair hydroxylase activity would also impact the role of JMJD5 in replication fidelity. To
145 test this, we focussed on six JMJD5 cancer variants that were expressed normally but had
146 reduced activity (S241L, Y262C, P319L, D323N, Q362H and W414R) (Figure 2B-C). These
147 mutants were cloned into a doxycycline-inducible lentiviral vector for conditional re-expression
148 following JMJD5 knockdown (because our siRNA sequences target the JMJD5 mRNA 3'UTR,
149 the reconstituted cDNAs are resistant to knockdown). First, we confirmed successful
150 knockdown of endogenous JMJD5 and reconstitution of exogenous wildtype JMJD5, an
151 inactive mutant (H321A), or the JMJD5 cancer variants (Figure 2D). Next, we tested the ability
152 of the cancer variants to prevent replication stress induced by endogenous JMJD5
153 knockdown. As hypothesized, cancer variants that reduced JMJD5 hydroxylase activity were
154 also unable to restore normal levels of 53BP1 bodies (Figure 2E) or micronuclei (Supplemental
155 Figure 4).
156

157 **The role of JMJD5 in replication fidelity is epistatic with its interactor, RCCD1**

158 How JMJD5 inactivation causes replication stress in tumour cells, and whether it acts in
159 isolation, or as part of a wider complex or pathway, is not yet clear. To begin exploring this,
160 we initially considered the involvement of known JMJD5 interacting proteins. Previous studies
161 have shown that JMJD5 interacts with 'RCC1 domain-containing protein 1' (RCCD1) [20, 21],
162 a poorly characterised seven-bladed β-propeller protein. Like JMJD5, RCCD1 has also been
163 implicated in a variety of cancer types [22-25]. To investigate whether RCCD1 might act in the
164 same cellular pathway as JMJD5, we first tested whether RCCD1 depletion also caused
165 replication stress. RCCD1 knockdown in A549 (Figure 3A-C) and U2OS (Supplemental Figure
166 5) caused an increase in 53BP1 bodies and micronuclei. Furthermore, single molecule DNA
167 fibre analysis demonstrated that RCCD1 depletion increased fork stalling and asymmetry in
168 both the absence (Figure 3D-E) and presence (Supplemental Figure 6) of HU. Similar results
169 were obtained in U2OS cells (Supplemental Figure 7).
170

171 To test if JMJD5 and RCCD1 act in the same pathway controlling replication fidelity, we first
172 aimed to explore their epistatic relationship to one another following single or combined siRNA
173 knockdown (Figure 3F). We observed that simultaneous knockdown of JMJD5 and RCCD1 in
174 A549 cells did not increase levels of 53BP1 bodies, micronuclei, stalled forks, or fork
175 asymmetry, beyond that observed with single knockdown (Figure 3G-J). Similar results were

176 obtained for 53BP1 bodies and micronuclei in U2OS cells (Supplemental Figure 8). Overall,
177 these observations indicate that JMJD5 and RCCD1 likely act in the same pathway to maintain
178 replication fidelity.
179
180 Whilst validating knockdowns in the epistasis experiments described above, we also noticed
181 a potential inter-dependency in JMJD5 and RCCD1 protein expression. In A549 cells we
182 observed that JMJD5 siRNA knockdown resulted in reduced RCCD1 expression (Figure 3F),
183 whilst in U2OS cells we noticed a reduction in JMJD5 expression following RCCD1 siRNA
184 knockdown (Supplemental Figure 8). These observations, coupled with the apparent epistatic
185 relationship outlined above, led us hypothesise that JMJD5 and RCCD1 are obligate binding
186 partners that need to act in a complex together for optimal expression and function in
187 replication fidelity. To explore this further, we first characterised the JMJD5:RCCD1 interaction
188 in more detail.
189
190 **JMJD5 and RCCD1 form a stoichiometric 1:1 heterodimer dependent on key**
191 **electrostatic interactions**
192 We began by overexpressing JMJD5 in the presence or absence of overexpressed
193 RCCD1, observing that co-expression of RCCD1 increased the levels of JMJD5 (Figure 4A).
194 Furthermore, Coomassie staining of SDS-PAGE gels following co-immunoprecipitation
195 demonstrated that JMJD5 and RCCD1 form a stable complex (Figure 4B) and a partially
196 purified complex eluted as a single peak with an apparent molecular weight of ~90kDa
197 consistent with the formation of a 1:1 heterodimer between JMJD5 (~47kDa) and RCCD1
198 (~40kDa) (Supplemental Figure 9)
199
200 Available empirical structural information for these proteins is currently limited to X-ray
201 structures of the Jmjd5 catalytic domain[12]. To identify amino acids that mediate
202 JMJD5/RCCD1 binding we used AlphaFold to generate a model of the complex (Figure 4C).
203 Within this predicted structure, the catalytic domain (CD) closely resembles that of extant
204 crystal structures with a core double stranded β-helix (DSBH) that forms the active site cleft,
205 elaborated by the classical N-terminal extension (NTE) that wraps around and extends the
206 DSBH sheet. Consistent with our earlier modelling studies [13], the JMJD5 N-terminal domain
207 (NTD) forms a helical stack structure reminiscent of tetratricopeptide repeats (TPR). Its two
208 C-terminal helices (α4/5) pack exclusively against the CD N-terminal extension through
209 contributing to a wedge-shaped arrangement for the full-length enzyme. As expected from its
210 sequence homology with RCC1 [26], RCCD1 adopts a 7-bladed β-propellor architecture and
211 interacts with α2 of the JMJD5 NTD through a surface centred on an unusual cluster of

212 exposed Trp residues (Figure 4C) through a largely hydrophobic interface further stabilised by
213 electrostatic/salt-bridging interactions between D73 and E77 from JMJD5 and R310 and K328
214 on RCCD1 (Figure 4D).
215
216 Supporting the veracity of the AlphaFold model, substitution of either D73 or E77 significantly
217 reduced the interaction of JMJD5 with RCCD1 in co-IP assays, whilst a D73A/E77A double
218 mutant completely ablated binding (Figure 4E). To test the impact of mutating the
219 corresponding residues in RCCD1, we used methionine substitutions to maintain hydrophobic
220 packing of the aliphatic portions of the R310 and K328 side-chains against surface-exposed
221 Trp residues, W220 and W326 respectively. Consistent with the AlphaFold predictions, an
222 R310M/K328M mutant completely blocked the interaction of RCCD1 with JMJD5 (Figure 4F).
223 Overall, these and previous observations validate the structural prediction and confirm the
224 critical contribution of electrostatic interactions to JMJD5:RCCD1 complex stability.
225
226 Disruption of critical interactions in tumour suppressor complexes can be positively selected
227 during cancer development. If the interaction of JMJD5 and RCCD1 is essential for
228 maintaining replication fidelity and suppressing tumourigenesis, we hypothesised that some
229 of the interacting residues identified above would be mutated in tumour samples and that these
230 would disrupt the JMJD5:RCCD1 interaction. Interrogating the cBioPortal and COSMIC
231 databases identified a JMJD5 E77K mutation in a malignant melanoma sample that would be
232 predicted to disrupt one of the critical electrostatic interactions with RCCD1. Other cancer
233 mutants were also identified in close proximity to D73 and E77 (V70L, S75F and L79P)
234 (Supplementary table 1). Whereas V70L and S75F substitutions did not impact the
235 JMJD5:RCCD1 interaction under the conditions tested, the L79P and E77K variants did
236 (Supplemental Figure 10). Similarly, we identified RCCD1 missense substitutions in residues
237 that are critical for the JMJD5 interaction, including R310W/Q (Ewings Sarcoma and Skin
238 Squamous Cell Carcinoma) and K328N (uterine carcinoma) (Supplementary Table 3). The
239 R310W and K328N mutations significantly compromised the ability of JMJD5 to interact with
240 RCCD1 (Supplemental Figure 10).
241
242 These data suggest that critical determinants of the JMJD5:RCCD1 interaction predicted from
243 the AlphaFold model may be altered in human tumours, thus highlighting the importance of
244 understanding the function of the JMJD5:RCCD1 in greater detail.
245
246 **JMJD5:RCCD1 complex formation is essential to maintain replication fidelity in tumour**
247 **cell lines**

248 Having identified experimental and disease mutants that disrupt the JMJD5:RCCD1
249 interaction, we next sought to leverage these to test the importance of complex formation for
250 maintaining replication fidelity in tumour cells, initially focussing on the JMJD5 D73A/E77A
251 mutant. To do so, we moved to the 'rescue' system described above. Western blot analyses
252 confirmed successful knockdown and re-expression of wildtype and H321A JMJD5, although
253 comparable re-expression of the D73A/E77A mutant required a 100-fold higher doxycycline
254 concentration (consistent with the importance of the RCCD1 interaction for JMJD5 expression)
255 (Figure 5A). Whereas reconstitution with wildtype JMJD5 was able to fully restore control
256 levels of 53BP1 bodies (Figure 5B), the D73A/E77A RCCD1-binding mutant was not, behaving
257 more similarly to the functionally inactive H321A mutant. Quantification of other replication
258 stress markers confirmed that reconstitution with D73A/E77A JMJD5 was unable to restore
259 control levels of micronuclei (Supplemental Figure 11), stalled forks (Figure 5C) or fork
260 asymmetry (Figure 5D).
261
262 To test if the reciprocal was also true, we generated A549 cells constitutively expressing
263 wildtype RCCD1 or the JMJD5 binding mutant R310M/K328M (Figure 5E). Similarly to the
264 D73A/E77A JMJD5 mutant reconstitution experiments above, the R310M/K328M mutant was
265 less well expressed than wildtype RCCD1, consistent perhaps with the importance of the
266 interaction with JMJD5 for optimal protein expression. Despite the reduced expression of the
267 R310M/K328M mutant from this constitutive vector, we noted it was still expressed to similar
268 or slightly higher levels than endogenous RCCD1 (Figure 5E). Therefore, we reasoned it could
269 still be used to restore physiological levels of RCCD1 expression that could be used to test
270 the functional competence of this mutant. Whereas wildtype RCCD1 was able to restore
271 replication stress markers to control levels, the JMJD5 binding mutant was not (Figure 5F-H
272 and Supplemental Figure 12).
273
274 Although our data demonstrates a clear role for JMJD5:RCCD1 complex formation in
275 maintaining replication fidelity in tumour cells, the precise nature of its role requires further
276 investigation.
277

278 **The JMJD5:RCCD1 complex interacts with HR factors and is required for restart of**
279 **stalled replication forks**

280 To explore the role of JMJD5 and RCCD1 in replication fidelity and human disease in more
281 detail, we were motivated to identify their most proximal biology using mass spectroscopy
282 (MS)-based interactomics. Early attempts using single JMJD5 or RCCD1 pulldowns did not
283 yield high fidelity assignment of nuclear proteins known to play a role in replication or

284 associated biology. In light of this, and our findings demonstrating the critical importance of
285 the JMJD5:RCCD1 interaction for their function, we reasoned that new proteomic screens
286 were warranted using the JMJD5:RCCD1 complex as bait. To this end we used a multicistronic
287 doxycycline-inducible vector containing HA-JMJD5 and RCCD1-FLAG cDNAs separated by a
288 P2A sequence to generate two separately expressed proteins that we confirmed formed a 1:1
289 complex (Supplemental Figure 13).

290 Next, we considered the need to enrich for relevant JMJD5:RCCD1 interactors by treating
291 cells with a relevant stressor. We opted for a prolonged HU treatment because it induces
292 replication stress and DNA damage that activates homologous recombination (HR) [27]. The
293 rationale for this was that, in addition to its role in replication fidelity, JMJD5 has also been
294 implicated in the late stages of HR [28], similar to several other factors implicated in both the
295 RS and DNA damage responses [29]. MS/MS sequencing of large-scale anti-FLAG
296 immunoprecipitations under these conditions identified more than fifty proteins that were
297 specific to JMJD5:RCCD1 pulldowns and that met our filtering criteria (Supplementary Table
298 4). To triage the hits, we screened the candidates for HR and/or replication factors and
299 identified two RAD51 paralogues known as RAD51C and XRCC3. RAD51C and XRCC3 form
300 a complex known as CX3 which has been implicated in late-stage HR [30] and replication fork
301 restart [31]. Independent co-immunoprecipitation experiments in HEK293T cells following 24
302 hours of HU treatment confirmed that JMJD5:RCCD1 interacts specifically with RAD51C and
303 XRCC3, but not RAD51, other RAD51 paralogues (RAD51B), or RPA (Figure 6A). Purified
304 JMJD5:RCCD1 complex also interacted specifically with recombinant CX3 complex *in vitro*
305 (Supplemental Figure 14).

306 The CX3 complex has an important role in replication fork restart [31]. This raised the
307 possibility that the function of the JMJD5:RCCD1 complex in replication fidelity and disease
308 might be related to restarting stalled replication forks. To investigate this, we used a modified
309 version of the DNA fibre assay (Figure 6B) [31]. Consistent with our hypothesis, siRNA
310 knockdown of either JMJD5 (Figure 6C) or RCCD1 (Figure 6D) caused a significant increase
311 in stalled forks, which in this assay indicates a deficit in replication fork restart. We next
312 engaged our JMJD5 and RCCD1 reconstitution models, noting that both formation of the
313 JMJD5:RCCD1 complex (Figure 6E and 6F) and the catalytic activity of JMJD5 (Figure 6E)
314 are essential for replication fork restart.

315 Our earlier study reporting the role of JMJD5 in replication fidelity followed the identification of
316 JMJD5 loss-of-function variants as the causal basis of a novel neurodevelopmental disorder
317 [13]. In light of our findings in tumour cell lines, we considered the possibility that replication
318 fork restart was also defective in our neurodevelopmental disorder patients. Primary cells
319 derived from an affected patient carrying biallelic inactivating JMJD5 variants displayed a

deficit in replication fork restart (Supplemental Figure 15), which could be rescued by reconstitution of catalytically active JMJD5 (Figure 6G).

Finally, we tested the hypothesis that JMJD5, RCCD1, and CX3 function in the same pathway in replication fork restart using epistasis analysis. Knockdown of XRCC3 was used to selectively inhibit the CX3 complex, as reported previously [31] (Supplemental Figure 16). Interestingly, co-depletion of either RCCD1/XRCC3 or JMJD5/XRCC3 did not exacerbate the replication fork restart deficit beyond that observed following knockdown of each factor in isolation (Figure 6H). This suggests that both heterodimeric complexes, JMJD5:RCCD1 and RAD51C:XRCC3, act in the same pathway controlling replication fork restart, and that this pathway underlies our observations of a role of the JMJD5:RCCD1 complexes in replication fidelity, neurodevelopmental disorders, and cancer.

Discussion

The findings presented here build on our prior work (REF patient paper) to further evidence the importance of the JMJD5 hydroxylase in human health and disease. We show that JMJD5 variants identified in human tumours impair protein expression (Figure 2B), and enzymatic activity (Figure 2C), and demonstrate that JMJD5 function is required to maintain replication fidelity in tumour cell lines (Figure 2E). We additionally demonstrate that JMJD5 forms a heterodimer with a cancer-associated seven-bladed β-propeller protein called RCCD1 (Figure 4), which we show also maintains replication fidelity. Critically, the role of RCCD1 in replication is dependent on its interaction with JMJD5 (Figure 3 and 5). Proteomic pulldowns using the JMJD5:RCCD1 complex identified a novel interaction with the RAD51 paralogue CX3 complex in tumour cell lines (Figure 6A), which led to us uncover an epistatic relationship between these two enigmatic complexes in replication fork restart (Figure 6H). Together with our observation of defective replication fork restart in JMJD5 patient cells (Figure 6G and Supplemental Figure 15), our work has the potential to unify the role of the JMJD5:RCCD1 complex in neurodevelopmental disorders and cancer.

The disruption of the JMJD5:RCCD1 interaction by damaging cancer-associated mutations (Supplemental Figure 10) suggests a previously unrecognised tumour suppressor axis involving a protein hydroxylase which, as an enzyme class, has not previously been widely studied in the context of cancer. Although the frequency of JMJD5 and RCCD1 *missense mutations* across all cancers appears relatively low, the full extent of JMJD5:RCCD1 functional inactivation in tumours is not yet known. Future work will address this by investigating alternative mechanisms of JMJD5:RCCD1 inactivation including, for example, copy number variation, epigenetic silencing, single nucleotide polymorphisms (SNPs) in transcription

355 regulatory sequences, aberrant mRNA splicing, and functional inactivation of the proteins
356 themselves.

357 Through a series of genome-wide and transcriptome-wide association studies, RCCD1 has
358 been independently proposed as a novel TSG. A genome wide association study identified a
359 novel SNP (rs2290203) located in an intron of a gene 5,712 bp downstream of *RCCD1* [32],
360 which correlated with reduced RCCD1 mRNA expression and increased breast cancer risk.
361 Additional RCCD1-associated SNPs at the *15q26.1* genome location have been reported in
362 ovarian cancer (rs8037137) [25], breast cancer (rs3826033, rs2290202 and rs17821347) [23]
363 and pancreatic cancer (rs8028409) [33], all of which correlate with reduced mRNA expression
364 and increased disease risk.

365 Similarly, [34] identified risk variants in which increased RCCD1 expression correlated with a
366 reduced risk of breast cancer. Whether the reduced RCCD1 expression in these contexts
367 causes reduced JMJD5 protein expression (as reported here, Figure 4) and function, and the
368 potential impact of this on replication fork restart and genome stability, is not yet clear.

369 The tumour microenvironment has the potential to also impair JMJD5:RCCD1 function, given
370 the unique cofactor and nutrient dependencies of 2OG oxygenases [35]. Oncometabolites
371 such as fumarate, succinate, and D-2-hydroxyglutarate (D-2HG) produced by mutations in FH,
372 SDH, and IDH1/2, respectively, can competitively inhibit 2OG oxygenases due to their
373 structural similarity to 2OG [5]. This raises the possibility that JMJD5 activity may be similarly
374 compromised in metabolically reprogrammed tumours.
375

376 Hypoxia represents another potential mechanism of JMJD5 inactivation. While HIF prolyl
377 hydroxylases are well-characterised oxygen sensors, the oxygen sensitivity of JmjC-only
378 hydroxylases such as JMJD5 remains poorly defined [5]. Of interest to the work presented
379 here, and the potential oxygen-sensitivity of JMJD5, hypoxic stress is known to suppress
380 homologous recombination, impair DNA replication, and promote genomic instability [36].
381 Whether JMJD5 inhibition contributes to hypoxia-induced replication defects remain to be
382 determined, but our findings suggest this is a promising avenue for future investigation with
383 broad clinical relevance.
384

385 Whilst the evidence presented here demonstrates a clear role for the JMJD5:RCCD1
386 heterodimer in replication fidelity (Figure 4 and 5), further work is required to uncover the
387 precise role of each protein. For example, the presence of RCCD1 raises questions about its
388 potential role in regulating JMJD5 catalytic activity, substrate binding, and subcellular
389 localisation. To lay the groundwork for detailed future investigation of these possibilities, we
390 identified the interactome of the JMJD5:RCCD1 complex, for the first time, by developing and

391 applying a P2A-based dual expression system (Figure 6). The novel interaction we describe
392 between the JMJD5:RCCD1 and CX3 heterodimers (Figure 6) may be consistent with a role
393 in a specific aspect of replication fork biology. CX3 is one of two separate RAD51 paralog
394 complexes that also include 'BCDX2'. Whereas CX3 plays a role in replication fork restart, as
395 described above, BCDX2 is required for replication fork reversal [31]. The absence of RAD51B
396 in JMJD5:RCCD1 pulldowns (Figure 6) suggests the interaction with RAD51 paralogs is
397 specific to CX3, pointing to a role for JMJD5:RCCD1 in replication fork restart over reversal.
398 Consistent with this, we did not observe a decrease in replication fork speed in JMJD5 mutant
399 patient cell lines [13], which would ordinarily be indicative of a defect in replication fork reversal
400 [37]. Rather we observed that JMJD5, RCCD1 and, importantly, the interaction between them,
401 is required for replication fork restart consistent with a potential functional relationship with the
402 CX3 complex. In line with this, we demonstrate that the JMJD5:RCCD1 and CX3 heterodimers
403 are epistatic to one another with respect to defective replication fork restart (Figure 6). Beyond
404 replication fork restart, the CX3 complex also plays an important role in DNA damage repair
405 through the Homologous Recombination (HR) pathway [30, 38]. Therefore, the interaction with
406 CX3 may also suggest a potential role for the JMJD5:RCCD1 complex in HR. Interestingly,
407 JMJD5 loss of function has been shown to hypersensitise to ionising radiation and delay the
408 resolution of RAD51 foci in C. elegans [28, 30], which aligns with similar phenotypes observed
409 following CX3 depletion in other models [30]. Future work will focus on understanding the
410 biochemical relationship between CX3 and JMJD5:RCCD1 in more detail, including whether
411 this relates to the hydroxylase activity of JMJD5, and the molecular mechanism by which this
412 regulates replication fork restart and HR.
413
414 The identification here of a novel cancer-associated pathway raises the possibility of
415 developing new therapeutic approaches. We recently developed novel JMJD5 inhibitors and
416 demonstrated that they cause increased replication stress in tumour cell lines [39], consistent
417 with the importance of JMJD5 catalytic activity for replication fidelity and genome stability
418 (Figure 2 and [13]). Inhibition of factors involved in these and related cellular processes often
419 sensitises cells to genotoxic agents. Indeed, RAD51C and XRCC3 loss-of-function can
420 sensitise tumour cells to a variety of genotoxic agents including PARP inhibitors and Cisplatin
421 [40, 41]. It will, therefore, be of interest to determine whether inactivation of the JMJD5:RCCD1
422 complex, be that genetic, chemical, or biochemical, also sensitises tumour cells to genotoxic
423 agents, and whether combination therapies might provide an additional new therapeutic
424 opportunity.
425
426 In line with our evidence for damaging JMJD5:RCCD1 mutations in tumours, reports of
427 reduced RCCD1 expression being linked to cancer predisposition, and the functional and

428 physical interaction of JMJD5:RCCD1 with the CX3 complex, both RAD51C and XRCC3 have
429 been implicated in cancer susceptibility and tumourigenesis [42-45]. Additionally, defects in
430 the RAD51C component of the CX3 complex are the basis of the developmental disorder
431 Fanconi Anaemia [42]. Whilst our previously reported clinical and cellular phenotypes for
432 patients affected by damaging JMJD5 variants are not directly analogous to Fanconi Anaemia,
433 they are both congenital disorders underpinned by increased genome instability [13, 42]. Our
434 combined biochemical, clinical and functional data would predict that inherited variants that
435 impair RCCD1 function (or other as yet unknown components of the pathway) may be the
436 cause of some undiagnosed neurodevelopmental disorders.
437
438 In summary, we have provided further evidence of the disease relevance of the protein
439 hydroxylase JMJD5, identifying other key members of a potential new tumour suppressor
440 pathway involving RCCD1, RAD51C and XRCC3. In doing so, we have significantly expanded
441 our knowledge of JMJD5 biology, and that of protein hydroxylases more broadly. Our work
442 also highlights the potential importance of 'obligate' binding partners for the function of JmjC-
443 hydroxylases, in this case RCCD1 and its role in the restart of stalled replication fork. The work
444 supports the increasing evidence that JmjC-only 2-OG oxygenases are key modulators of
445 human disease progression that warrant further investigation in both the discovery and
446 translational research spaces.
447

448 ## Materials and Methods

449 ### DNA expression vectors

450 N-terminally HA epitope-tagged JMJD5 in pEF6 was generated as previously described [13].
451 N-terminally FLAG epitope-tagged doxycycline-inducible JMJD5 expression vectors, were
452 created by PCR subcloning into modified lentiviral pTRIPZ (Dharmacon) vectors, in which the
453 RFP cDNA was replaced with a modified multiple cloning site (termed pTIPZ, a gift from
454 Matthew Cockman, Francis Crick Institute, London, UK). N-terminally glutathione S-
455 transferase-tagged (GST-tagged) pGEX-4T-1 JMJD5 was generated as previously described
456 [13]. C-terminally HA epitope-tagged RCCD1 expression vector was generate by cloning
457 human *RCCD1* open reading frame (ORF) by PCR using Phusion High Fidelity DNA
458 Polymerase (New England Biolabs) into pcDNA3.1 (Thermo Fisher). Lentiviral C-terminally
459 FLAG-epitope tagged RCCD1 expression vector was generated by PCR subcloning into
460 modified pGIPZ in which the GFP cDNA was replaced with a limited multiple cloning site and
461 the puromycin resistance cDNA was replaced with hygromycin resistant cDNA (termed pIHZ;
462 gift from Tencho Tenev, Institute of Cancer Research, London, UK). Both pEF6 HA-JMJD5

463 and pcDNA3.1 RCCD1-HA were used as templates for site-directed mutagenesis PCR
464 reactions as previously described [13]. Following SDM PCR, successful RCCD1 clones were
465 subcloned into pIHZ as above. The DNA sequence for HA-JMJD5-P2A-RCCD1-3XFLAG was
466 commercially ordered from TransOmic and cloned into pTIPZ via restriction cloning.

467

468 **Cell treatments**

469 siRNA transfections were performed using Lipofectamine RNAiMAX (Invitrogen) according to
470 manufacturer's instructions. All siRNAs were used at a working concentration of 30 nM. siRNA
471 oligonucleotides were purchased from Sigma-Aldrich (Supplemental Figure 17). Control
472 transfections were carried out using a negative control siRNA (Sigma-Aldrich SIC001), as
473 previously described [13]. DNA plasmid transfection was performed using FuGENE
474 (Promega) according to the manufacturer's instructions. N-terminally FLAG epitope-tagged
475 JMJD5 expression was induced using doxycycline, 24 hours after plating of stable cell lines.
476 Concentration and duration of doxycycline treatment is indicated for each experiment. 1 mM
477 hydroxyurea treatment was used where indicated.

478

479 **Cell culture**

480 A549 (CCL-185), HeLa (CLL-2) and HEK293T (CRL-3216) cell lines were purchased from
481 ATCC. U2OS cells were a gift from Martin Higgs (University of Birmingham). All cell lines were
482 cultured in DMEM plus 10% (v/v) FBS (Sigma-Aldrich) and 1% penicillin/streptomycin in a
483 humidified environment at 37°C with 5% CO_2. Lentiviral transduced stable cell lines were
484 generated using FuGENE cotransfection of HEK293T with doxycycline-inducible JMJD5
485 cDNA, constitutively expressing RCCD1 cDNA or doxycycline-inducible HA-JMJD5-P2A-
486 RCCD1-3XFLAG cDNA (details above) plus psPAX2 and pMD2.G packaging vectors. The
487 lentiviral supernatant was filtered and incubated on the recipient cells before selection and
488 growth of successfully transduced cell lines in 1 µg/mL puromycin or 200 µg/mL hygromycin
489 as appropriate.

490

491 **Western blotting**

492 Whole cell extracts were prepared in RIPA (25 mM Tris-HCl pH 8, 150 mM NaCl, 0.5% (v/v)
493 sodium deoxycholate (SDS), 1% NP-40) or JIES (100 mM NaCl, 5mM $MgCl_2$, 20 mM Tris-HCl
494 pH 7.4, 0.5% (v/v) NP-40) with 1x SIGMAFAST protease inhibitor cocktail (Sigma-Aldrich).
495 Proteins were separated by SDS-PAGE using 12% (v/v) polyacrylamide gels. Samples were
496 subsequently transferred onto PVDF membranes (GE Healthcare) before immunoblotting with
497 the indicated antibodies (Supplemental Figure 17). All antibodies were sourced commercially
498 with the exception of mouse anti-JMJD5 which was a gift from Matsuura Yoshiharu (Osaka

499 University, Osaka, Japan). Chemiluminescent signal was developed using Clarity or Femto-
500 ECL (Bio-Rad) and visualised using a Fusion FX Vilber Imager. Coomassie staining was
501 carried out using Instant Blue (Sigma-Aldrich).
502
503 **Immunoprecipitation**
504 Whole cell extracts were prepared in JIES as above. An input fraction was taken and prepared
505 in 6x Laemmli buffer (125 mM Tris-HCl pH 6.8, 6% SDS (w/v), 50% glycerol (v/v), 225 mM
506 dithiothreitol (DTT), 0.1% (w/v) bromophenol blue. Anti-HA agarose (Sigma-Aldrich) or anti-
507 FLAG (Sigma-Aldrich) magnetic beads were added to the remaining whole cell lysates and
508 incubated rotating overnight at 4°C. The beads were then washed six times in JIES before
509 peptide elution using 100 µg FLAG (Generon) or HA (Sigma-Aldrich) peptide in 20 mM Tris-
510 HCl pH8 and 100 mM NaCl. The beads were incubated in elution buffer for 15 minutes at room
511 temperature with shaking at 1400 rpm. The resulting elution was prepared in 6x Laemmli buffer
512 and boiled at 95°C for 5 minutes.
513
514 **Mass spectrometry**
515 The HA-JMJD5:RCCD1-3XFLAG complex was anti-FLAG immunopurified from
516 overexpressing HEK293T P2A cells and eluted with 3XFLAG peptide. A control sample of
517 HEK293T cells expressing pTIPZ EV was included to identify non-specific interactors
518 associated with anti-FLAG immunoprecipitation. Samples were extracted, in-solution digested
519 with trypsin, desalted, and analyzed by mass spectrometry. Data were searched against the
520 UniProt Reference Homo sapiens database with PEAKS Studio X Software (Bioinformatics
521 Solutions). Cysteine carbamidomethylation was selected as a 'fixed' modification, with
522 oxidation (M) and deamidation (N, Q) as variable modifications. Resulting data was triaged as
523 follows, firstly any proteins identified in the control (EV) samples lacking HA-JMJD5:RCCD1-
524 FLAG were removed. We also removed proteins identified in 50% or more of the screens listed
525 in the 'Contaminant Repository for Affinity Purification' (CRAPome) [46]. The resulting top 50
526 were ranked by percentage coverage and presented in Supplementary Table 4.

527 **Recombinant JMJD5 protein**
528 pGEX-4T-1 JMJD5 was transformed into BL21(DE3)-competent cells (Promega) and
529 recombinant protein was generated as previously described [13].
530
531 ***In vitro* interaction assays**
532 *In vitro* interaction assays were performed by first using anti-FLAG immunoprecipitation as
533 described above. After the wash steps the anti-FLAG magnetic beads were resuspended in 1
534 mL of interaction buffer (100 mM NaCl and 20 mM Tris pH8). 2.5 µg of recombinant CX3

535 complex (gift from Steve West, Francis Crick Institute) was added to the samples and
536 incubated at 4°C rotating for 4 hours. Samples were then washed six times in interaction buffer
537 and eluted using 100 µg FLAG peptide as above (Immunoprecipitation).
538
539 ***In vitro* hydroxylation assay**
540 As previously described [13].
541
542 **Immunofluorescence**
543 Cells were grown on glass coverslips and fixed using 4% (v/v) paraformaldehyde (PFA) at
544 room temperature for 15 minutes. For 53BP1 staining, pre-extraction was performed as
545 previously described [13]. Cells were permeabilised using 0.1% (v/v) Triton X-100 for 10
546 minutes before blocking in 1% (w/v) BSA (Sigma-Aldrich) in PBS for 1 hour. Coverslips were
547 then stained with the indicated antibodies (Supplemental Figure 17), incubated in DAPI
548 (Invitrogen) for 10 minutes before mounting with ProLong Gold (Cell Signalling). Cells were
549 imaged using a Leica DM6000B.
550
551 **DNA fibre assay**
552 Progression of DNA synthesis was monitored using the DNA fibre assay as previously
553 described [13].
554 **Statistics**
555 Experiments with a minimum of three independent biological repeats were used for statistical
556 analysis and the statistical test used is indicated for each experiment. Graphpad Prism was
557 used to perform 1-way ANOVA and Kruskal-Wallis tests.
558 **Structural modelling**
559 The interaction between JMJD5 and RCCD1 was predicted using AlphaFold 3 [47]. Predicted
560 local distance difference tests (pLDDT) and interface predicted template modelling (iPTM) was
561 performed within AlphaFold 3 to provide information about the structural accuracy of the
562 generated models. The resulting predictions were analysed using Chimera X.
563
564 **Analytical gel filtration**
565 Cells expressing JMJD5-RCCD1 were washed twice with PBS and lysed in a buffer consisting
566 of 20 mM Tris pH 8.0, 100 mM NaCl, 5 mM $MgCl_2$, 0.5% (v/v) NP-40, EDTA-free protease
567 inhibitor tablets, and 0.1 % (v/v) turbonuclease. The cell lysate was then centrifuged at 1500
568 rpm for 5 min, with the supernatant then incubated overnight with 40 µL of Anti-FLAG M2
569 magnetic beads per 4 mL of cell lysate. Beads were centrifuged at 1500 rpm for 2 min and

570 subsequently washed 6 times in 20 mM Tris pH 8.0, 100 mM NaCl, 5 mM MgCl2, 0.5% (v/v)
571 NP-40. JMJD5-RCCD1 was eluted from the beads using 100 µg/mL FLAG peptide in 20 mM
572 Tris pH 8.0, 100 mM NaCl. The fractions containing JMJD5-RCCD1 were pooled and
573 concentrated before additional purification on a Superdex 200 10/300 gel filtration column (GE
574 Healthcare) equilibrated in 20 mM Tris pH 8.0, 100 mM NaCl, 0.5 mM TCEP. The peak
575 absorbance at 280 nm of JMJD5-RCCD1 was then compared to a set of protein standards of
576 known molecular weights to allow for Mw approximation.

577 **Multiple sequence alignment**

578 JMJD5 protein sequences used for evolutionary conservation analysis were identified through
579 BLAST searches of NCBI databases. Sequences were aligned in MEGAX using the MUSCLE
580 algorithm [48] and shaded using the Texshade LaTeX package.

581 **Illustration of JMJD5 mutation plot**

582 Somatic mutation data for JMJD5 was obtained from the COSMIC and cBioPortal databases
583 and imported into R for analysis. Amino acid substitutions and variant classifications were
584 cleaned and reformatted to extract the corresponding residue positions within the encoded
585 protein. Lollipop plot was generated using the *G3viz* package in R. Mutation sites were
586 mapped to a linear protein schematic, with lollipop stems and markers drawn from the
587 processed mutation table. Variant classifications were encoded by colour to distinguish
588 between mutation types. Plot appearance and layout were further refined using *ggplot2*.

589 ## Acknowledgements

590 T.J.K. was supported by an MRC-DTP award to T.J.K. and M.L.C. S.C.F., E.H. and U.B. were
591 funded by a Cancer Research UK Programme Foundation Award to M.L.C. (C33483/A2567).
592 S.J.S. was supported by a transitional award from the Francis Crick Institute (CR2019/003DK).
593 The work was also supported by an MRC project grant to M.L.C. and S.J.S (APP23111).

594

595 ## Author contributions

596 T.J.K. and S.C.F. designed and performed the cell biology experiments, analysed the resulting
597 data, and generated the corresponding figures. T.J.K. led studies into the role of RCCD1 in
598 replication fidelity in tumour cell lines, the JMJD5:RCCD1 interaction and its importance for
599 replication fidelity and replication fork restart, and proteomic screens that identified CX3.
600 S.C.F. led studies into the role of JMJD5 in replication fidelity in tumour cell lines, cancer
601 genetic analyses, JMJD5 activity assays, and replication stress analysis in cells reconstituted
602 with JMJD5 cancer mutants. T.J.K., S.C.F., and M.L.C wrote the manuscript. S.J.S. and G.H.

603 performed structural and biophysical analyses. M.L.C. co-designed the experiments and
604 directed the project with S.J.S., S.C.F., and T.J.K. All authors approved the final version of the
605 manuscript.

606

607 **Competing interests**

608 The authors declare no competing interests.

609

610 **Figure 1**

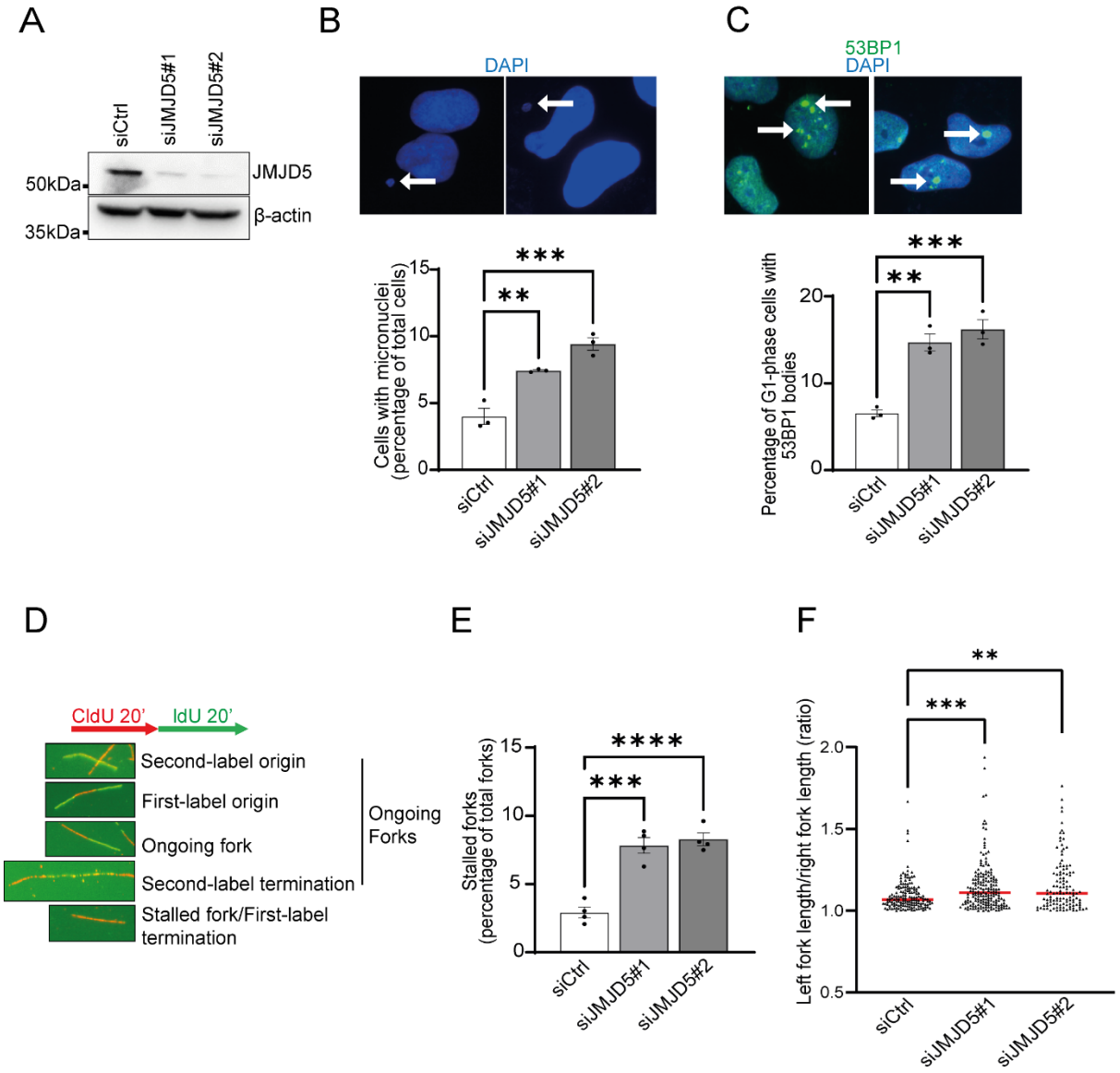

611

612 **Figure 1. JMJD5 maintains replication fidelity in tumour cell lines.** Lung adenocarcinoma
613 A549 were treated with siRNA before quantification of RS markers including micronuclei,
614 53BP1 bodies, stalled forks and fork asymmetry. **(A)** A549 cells were transfected with the
615 indicated siRNAs before western blot analysis to confirm JMJD5 knockdown. JMJD5
616 knockdown increased the number of **(B)** micronuclei and **(C)** 53BP1 bodies in G1 phase. **(D)**
617 Single molecule DNA fibre analysis was performed by incubating cells with thymidine
618 analogues CldU and IdU consecutively, before immunofluorescence detection (top).
619 Examples of different fibre structures are shown (bottom). Both **(E)** stalled forks and **(F)** fork
620 asymmetry was significantly increased following JMJD5 knockdown in A549 cells. Data
621 represent mean ± SEM from 3 **(B, C,** and **F)** or 4 **(E)** independent experiments. For 53BP1
622 bodies, a minimum of 300 cells were counted per sample. For micronuclei, a minimum of 500
623 cells were counted per sample. For stalled forks a minimum of 250 forks were counted per
624 condition per independent experiment. For fork asymmetry at least 50 structures were
625 measured per sample per independent experiment. Statistical analyses used 1-way ANOVA
626 with Bonferroni's post hoc test (**B, C,** and **E**) or Kruskal-Wallis with Dunn's correction (**F**); **P
627 ≤ 0.01, ***P ≤ 0.001, ****P ≤ 0.0001.
628

629 **Figure 2**

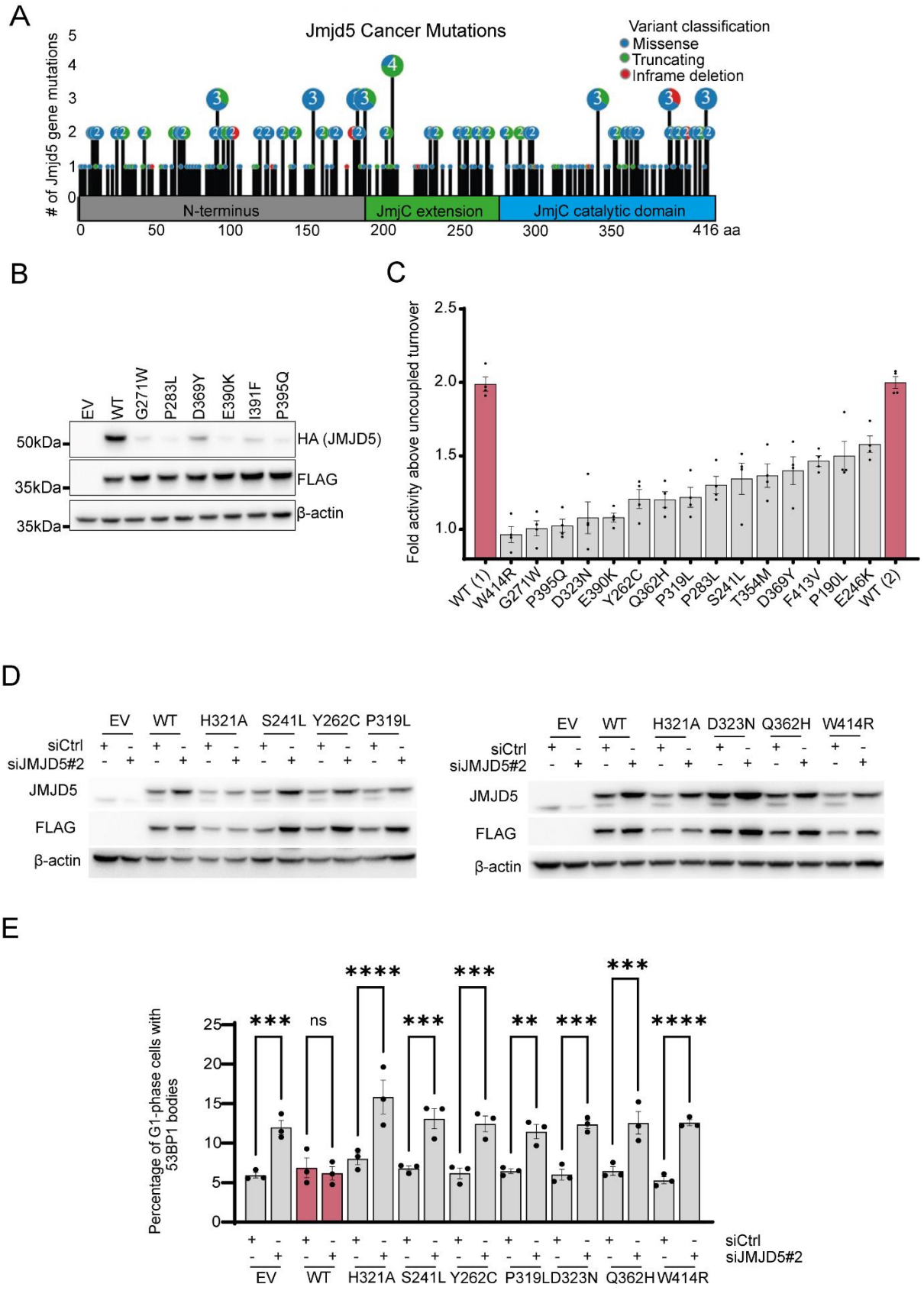

630

631 **Figure 2. *JMJD5* cancer mutations reduce expression, catalytic activity and impair**
632 **rescue of replication fidelity associated with JMJD5 knockdown. (A)** Full list of *JMJD5*
633 cancer mutations taken from online databases COSMIC and cBioPortal plotted against the

634 primary sequence of JMJD5. **(B)** HeLa cells were transfected with the indicated HA-JMJD5
635 constructs for 48 h and JMJD5 expression examined by western blotting. FLAG-JMJD7 was
636 used as a transfection control **(C)** GST-tagged WT JMJD5 and cancer variants were
637 expressed in *E. coli* and purified before in vitro activity assays. Activity was monitored using
638 the Succinate-Glo assay, which measures succinate production. Two separate WT
639 preparations were included in each assay for comparison. Data represent mean ± SEM from
640 4 independent experiments. All variants shown had a statistically significant reduction in
641 activity compared to WT JMJD5. **(D)** and **(E)** pTIPZ-FLAG JMJD5 A549 cell lines expressing
642 the indicated JMJD5 cancer variants were treated with 10 ng/mL doxycycline for one week
643 prior to transfection with siCtrl or siJMJD5#2. Cells were fixed after 72 h and 53BP1 bodies
644 quantified in G1 phase cells. Re-expression of WT JMJD5 reduced levels of 53BP1 bodies in
645 JMJD5 knockdown cells. In contrast, re-expression of the catalytically dead H321A mutant, or
646 cancer variants shown to affect JMJD5 activity were unable to reduce 53BP1 bodies. Data
647 represent mean ± SEM from 3 **(E)** or 4 **(B)** independent experiments. For 53BP1 bodies
648 analysis a minimum of 250 G1 phase cells were counted per sample in each experiment. **(D)**
649 western blot validation of JMJD5 reconstitution from panel **(E)**. Statistical analysis used 1-way
650 ANOVA with Bonferroni's post hoc test; ns not significant, **$P \leq 0.01$, ***$P \leq 0.001$, ****$P \leq$
651 0.0001.
652

653 **Figure 3**

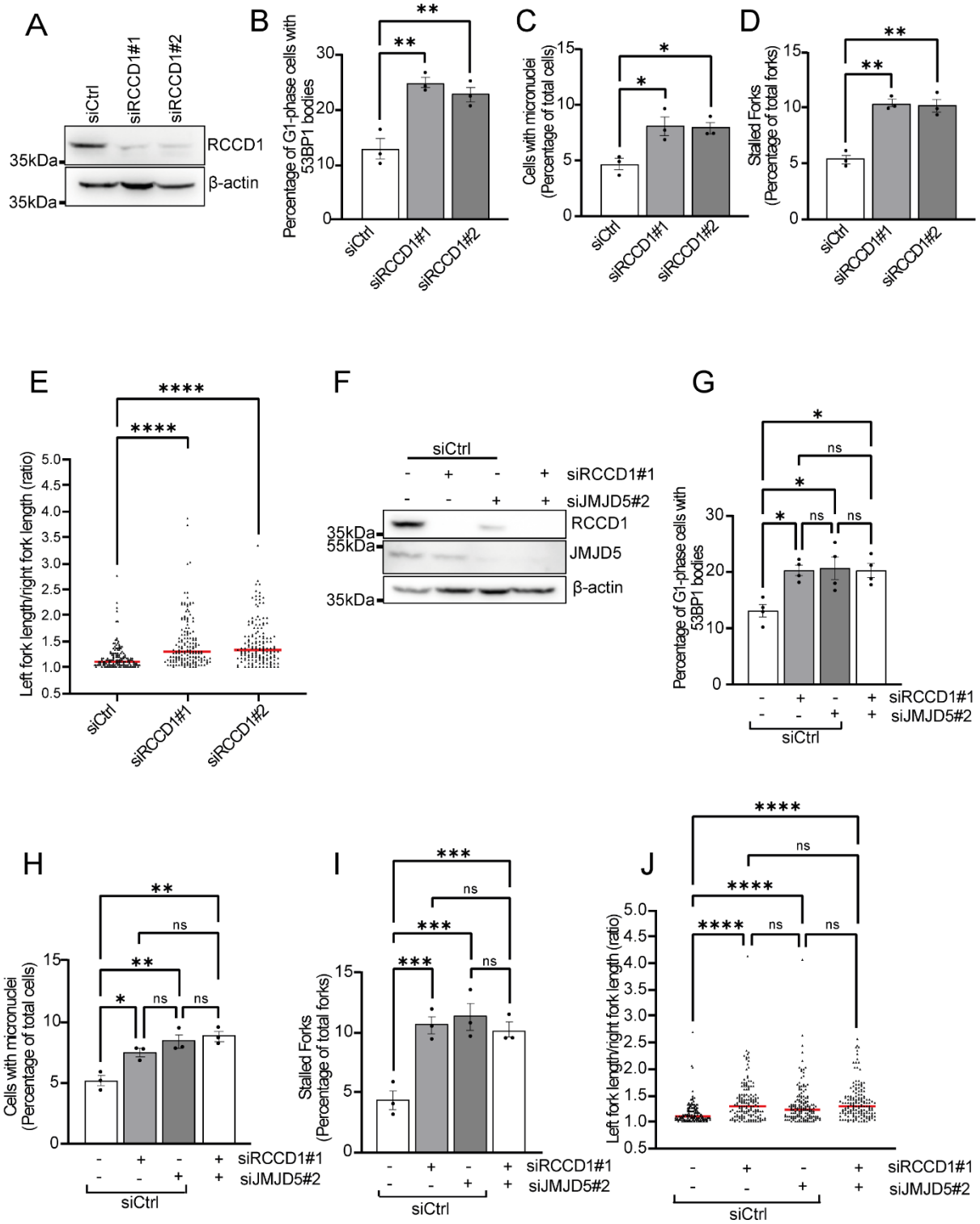

654 **Figure 3. RCCD1 depletion increases markers of replication stress epistatic with**
655 **JMJD5.** A549 cells were treated with siRNA and multiple markers of replication stress were
656 quantified including micronuclei, 53BP1 bodies, stalled forks and fork asymmetry. **(A)** A549
657 cells were transfected with indicated siRNAs and western blotted using the indicated
658 antibodies to confirm RCCD1 knockdown. siRNA knockdown of RCCD1 using two
659 independent sequences increased the number of **(B)** 53BP1 bodies, **(C)** micronuclei, **(D)**
660 stalled forks and **(E)** asymmetric forks. **(F)** Successful knockdown of JMJD5 and RCCD1 using
661 indicated siRNAs in A549 cells was confirmed via western blot. Cells were harvested 72 h

post transfection and analysed using the indicated antibodies. The JMJD5 and RCCD1 increased replication stress phenotypes are epistatic as indicated by no additional increase in **(G)** 53BP1 bodies, **(H)** micronuclei, **(I)** stalled forks and **(J)** fork asymmetry following concurrent knockdown. Data represent mean ± SEM from 3 **(B, C, D, E, H, I** and **J)** or 4 **(G)** independent experiments. For 53BP1 bodies, a minimum of 300 cells were counted per sample. For micronuclei, a minimum of 500 cells were counted per sample. For stalled forks a minimum of 250 forks were counted per condition per independent experiment. For fork asymmetry at least 50 structures were measured per sample per independent experiment. Statistical analyses used 1-way ANOVA with Bonferroni's post hoc test (**B, C, D, G, H** and **I**) or Kruskal-Wallis with Dunn's correction (**E** and **J**); *P ≤ 0.05, **P ≤ 0.01, ***P ≤ 0.001, ****P ≤ 0.0001.

674 **Figure 4**

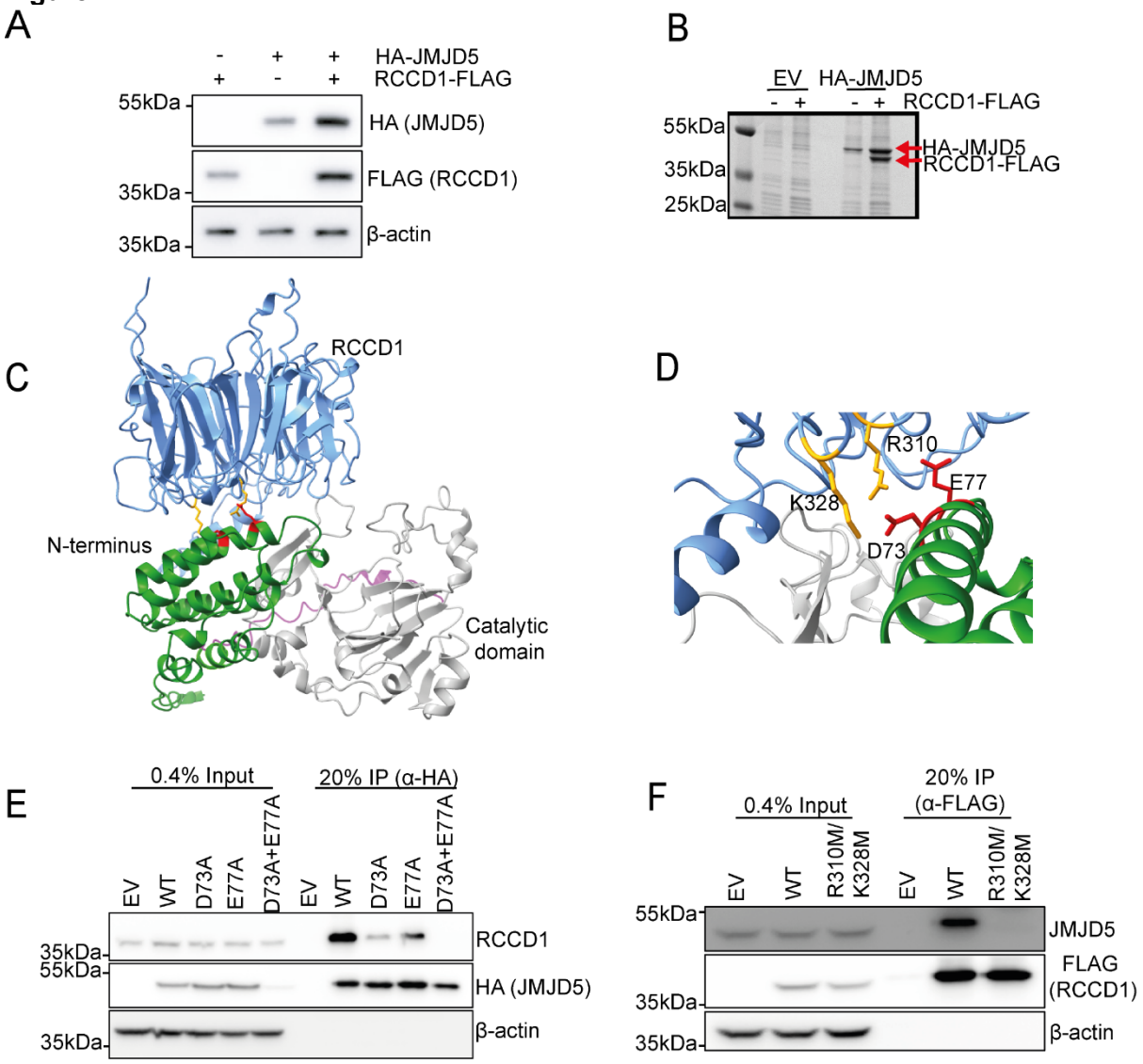

675
676 **Figure 4. JMJD5 and RCCD1 form a 1:1 heterodimer facilitated through D73A/E77A JMJD5. (A)** Expression of JMJD5 and RCCD1 is optimal when co-transfected. HEK293T cells
677 were transfected with either pIHZ RCCD1-FLAG, pEF6 HA-JMJD5, or both, before western
678 blotting with the indicated antibodies. **(B)** JMJD5 and RCCD1 form a stoichiometric 1:1
679 complex. HEK293T cells were transfected with indicated pEF6 constructs (EV or HA-JMJD5)
680 and pIHZ RCCD1-FLAG followed by anti-HA immunoprecipitation (IP). The
681 immunoprecipitated samples were then separated using SDS-PAGE and stained using
682 Coomassie. **(C)** AlphaFold3 prediction showed RCCD1 (blue) interacts with the N-terminus
683 (green) of JMJD5 which is connected to the catalytic domain (grey) through a flexible linker
684 (pink) **(D)** AlphaFold Multimer prediction supports the identification of JMJD5 D73/E77 (red)
685 and RCCD1 R310/K328 (orange) forming the binding interface between the two proteins. **(E)**
686 RCCD1 is unable to bind to JMJD5 D73A/E77A. Lysates from HEK293T cells transfected with
687 control pEF6 (EV), pEF6-HA-JMJD5(WT) or the indicated experimental alanine mutations
688 pEF6-HA-JMJD5(D73A, E77A or D73A+E77A) were subject to anti-HA immunoprecipitation
689 and western blotting with the indicated antibodies. **(F)** Experimental mutation of R310 and
690 K328 to methionine does reduce binding to JMJD5. Lysate from HEK293T cells transfected
691 with control pIHZ (EV), pIHZ-RCCD1-FLAG(WT) and pIHZ-RCCD1-FLAG(R310M/K328M)
692 were anti-FLAG immunoprecipitated (IP) followed by western blotting with the indicated
693 antibodies.
694
695

696 **Figure 5**

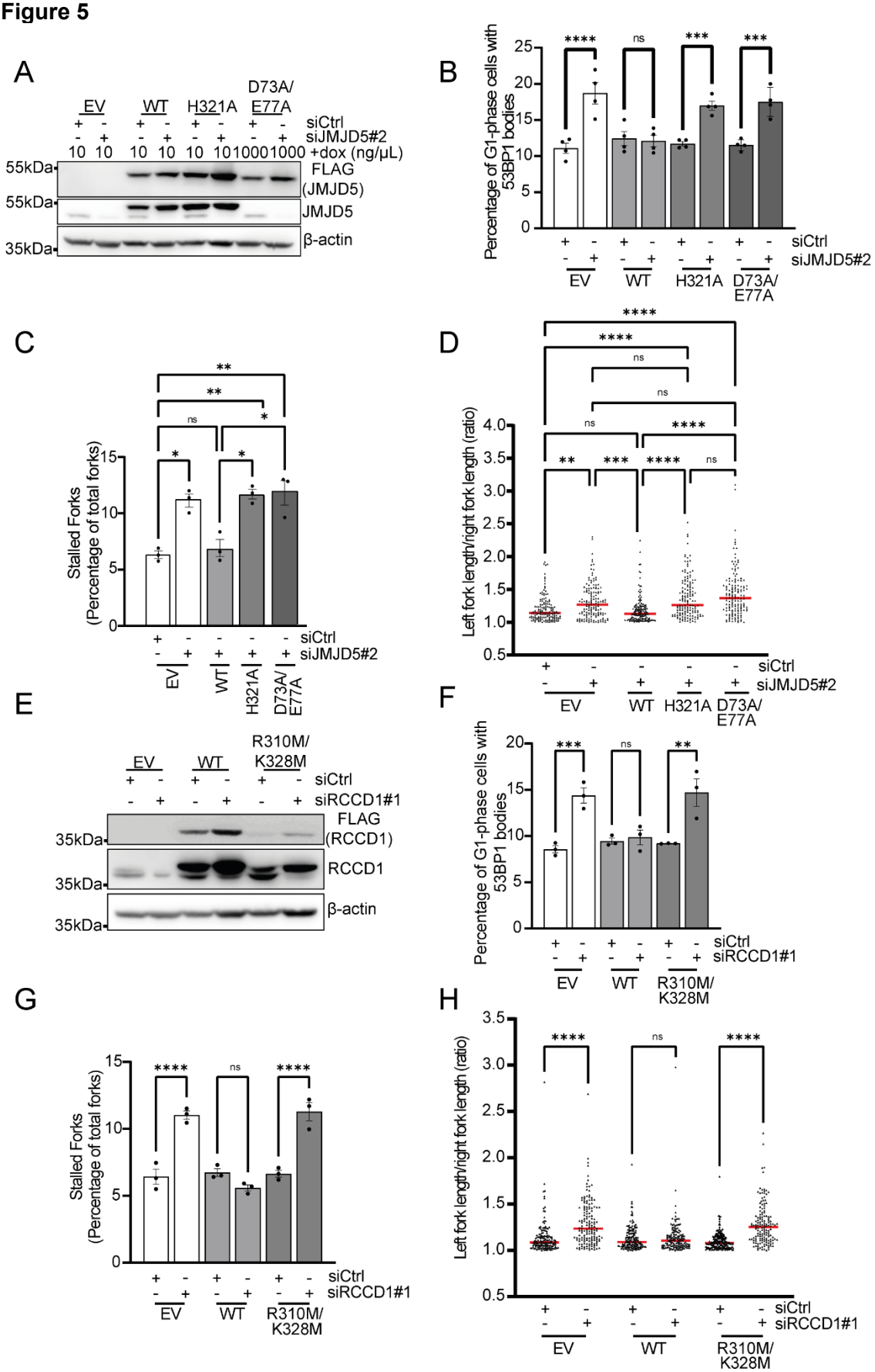

697

698 **Figure 5. JMJD5 and RCCD1 binding mutants are unable to rescue siRNA induced**
699 **increases in markers of replication stress.** pTIPZ-JMJD5 or pIHZ-RCCD1 A549 cells were

transfected with indicated siRNAs before quantification of 53BP1 bodies, stalled forks and fork asymmetry. **(A)** The indicated pTIPZ-JMJD5 A549 cell lines (EV, WT, H321A and D73A/E77A) were treated with indicated concentrations of doxycycline for one week prior to transfection with siCtrl or siJMJD5#2. Cells were harvested after 72h and JMJD5 knockdown was confirmed via western Blot with the labelled antibodies. Note that expression of D73A/E77A was not detected using the JMJD5 antibody as these mutations presumably destroy the antigen. pTIPZ-JMJD5 WT but not H321A or D73A/E77A was able to rescue increases in **(B)** 53BP1 bodies, **(C)** stalled forks and **(D)** fork asymmetry caused by siJMJD5. **(E)** pIHZ-RCCD1 (EV, WT, R310M/K328M) were transfected with the indicated siRNAs and knockdown of RCCD1 was confirmed via western Blot. pIHZ-RCCD1 WT but not the JMJD5 binding mutant R310M/K328M showed rescue of siRCCD1#1 induced increases in **(F)** 53BP1 bodies, **(G)** stalled forks and **(H)** fork asymmetry. Data represent mean ± SEM from 3 **(C, D, F, G and H)** or 4 **(B)** independent experiments. For 53BP1 bodies, a minimum of 300 cells were counted per sample. For stalled forks a minimum of 250 forks were counted per condition per independent experiment. For fork asymmetry at least 50 structures were measured per sample per independent experiment. Statistical analyses used 1-way ANOVA with Bonferroni's post hoc test (**B, C, F** and **G**) or Kruskal-Wallis with Dunn's correction (**D** and **H**); *P ≤ 0.05, **P ≤ 0.01, ***P ≤ 0.001, ****P ≤ 0.0001.

719 **Figure 6**

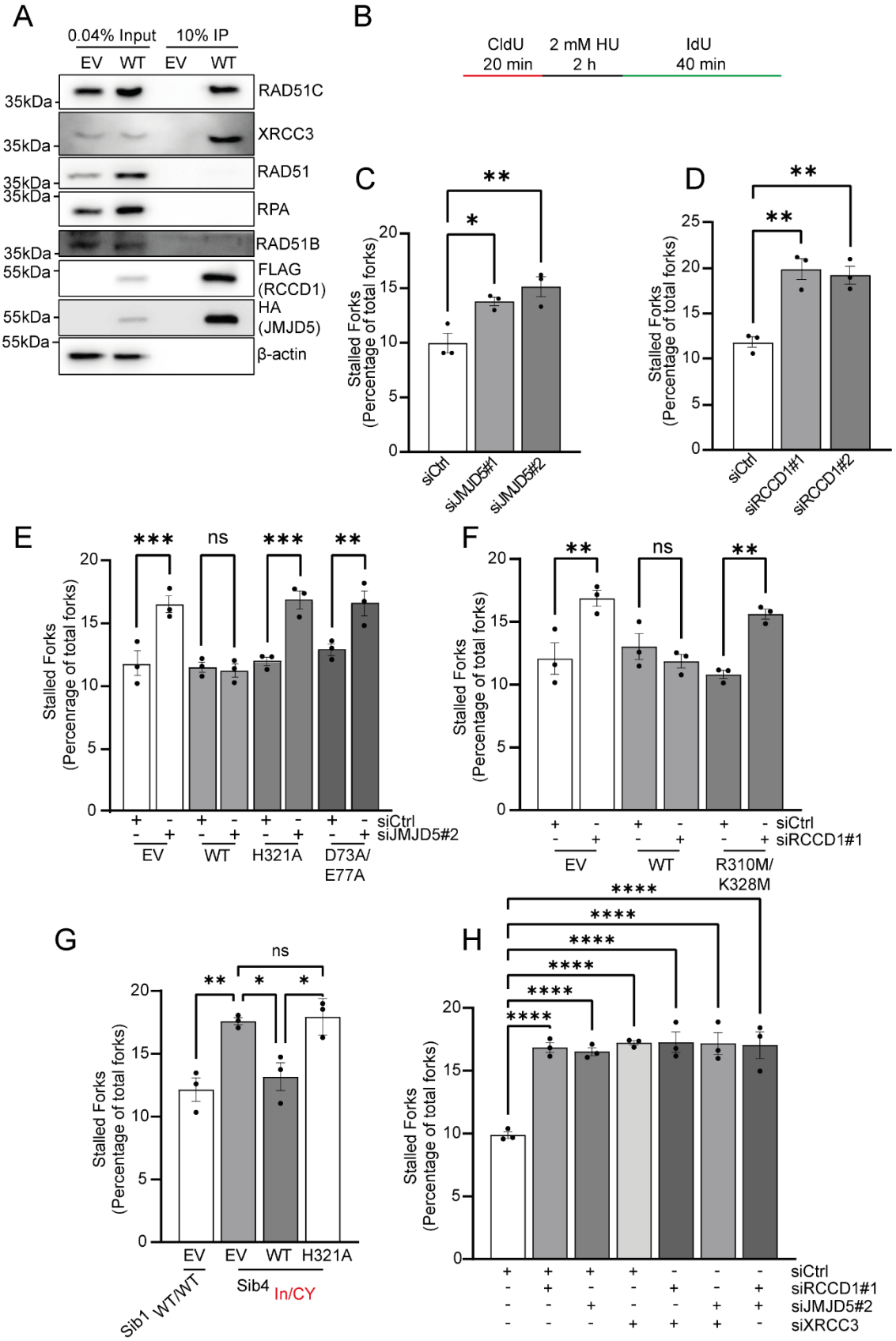

720

721 **Figure 6. The JMJD5:RCCD1 heterodimer interacts with the CX3 complex of RAD51**
722 **paralogs to facilitate normal restart of stalled replication forks. (A)** The JMJD5:RCCD1
723 heterodimer interacts with the CX3 complex of RAD51 paralogs. HEK293T cells expressing

doxycycline inducible pTIPZ EV or WT HA-JMJD5-P2A-RCCD1-3XFLAG were treated with doxycycline for 48 h before 2 mM HU treatment for 24 h. Resulting protein lysates were anti-FLAG immunoprecipitated (IP) followed by western blotting with the indicated antibodies. **(B)** Modified DNA fibre assay**.** To measure fork restart CldU/IdU was pulse-labelled for indicated times with HU treatment (2 mM, 2 h). siRNA knockdown of both **(C)** JMJD5 and **(D)** RCCD1 in A549 cells significantly increases the number of stalled forks associated with deficient replication fork restart. Formation of the JMJD5:RCCD1 heterodimer is required for restart of stalled replication forks with **(E)** Reconstitution of WT JMJD5 but not catalytically dead (H321A) or RCCD1 binding mutant (D73A/E77A) and **(F)** reconstitution of WT RCCD1 but not the JMJD5 binding mutant (R310M/K328M) able to rescue observed increases in HU induced deficient replication fork restart in A549 cells. **(G)** Reconstitution of active JMJD5 only in $Sib4_{In/CY}$ could rescue the observed increase in deficient replication fork restart. **(H)** Observed JMJD5/RCCD1 knockdown associated replication fork restart defects are epistatic with functional inactivation of the CX3 complex of RAD51 paralogs in A549 cells. For stalled forks associated with deficient replication fork restart a minimum of at least 50 structures were counted per condition per independent experiment. Data represents mean ± SEM from 3 **(C, D, E, F, G, and H)** independent experiments. Statistical analyses used 1-way ANOVA with Bonferroni's post hoc test **(C, D, E, F, G, and H).** *P ≤ 0.05, **P ≤ 0.01, ***P ≤ 0.001, ****P ≤ 0.0001. ns = non-significant.

1. Kivirikko, K.I. and D.J. Prockop, *Enzymatic hydroxylation of proline and lysine in protocollagen.* Proc Natl Acad Sci U S A, 1967. **57**(3): p. 782-9.
2. Islam, M.S., et al., *2-Oxoglutarate-Dependent Oxygenases.* Annu Rev Biochem, 2018. **87**: p. 585-620.
3. Kaelin, W.G., Jr. and P.J. Ratcliffe, *Oxygen sensing by metazoans: the central role of the HIF hydroxylase pathway.* Mol Cell, 2008. **30**(4): p. 393-402.
4. Martinez, S. and R.P. Hausinger, *Catalytic Mechanisms of Fe(II)- and 2-Oxoglutarate-dependent Oxygenases *.* Journal of Biological Chemistry, 2015. **290**(34): p. 20702-20711.
5. Fletcher, S.C. and M.L. Coleman, *Human 2-oxoglutarate-dependent oxygenases: nutrient sensors, stress responders, and disease mediators.* Biochem Soc Trans, 2020. **48**(5): p. 1843-1858.
6. Ploumakis, A. and M.L. Coleman, *OH, the Places You'll Go! Hydroxylation, Gene Expression, and Cancer.* Mol Cell, 2015. **58**(5): p. 729-41.
7. Bannister, A.J. and T. Kouzarides, *Regulation of chromatin by histone modifications.* Cell Res, 2011. **21**(3): p. 381-95.
8. Klose, R.J., E.M. Kallin, and Y. Zhang, *JmjC-domain-containing proteins and histone demethylation.* Nat Rev Genet, 2006. **7**(9): p. 715-27.
9. Johansson, C., et al., *The Roles of Jumonji-Type Oxygenases in Human Disease.* Epigenomics, 2014. **6**(1): p. 89-120.
10. Ishimura, A., et al., *Jmjd5, an H3K36me2 histone demethylase, modulates embryonic cell proliferation through the regulation of Cdkn1a expression.* Development, 2012. **139**(4): p. 749-59.
11. Hsia, D.A., et al., *KDM8, a H3K36me2 histone demethylase that acts in the cyclin A1 coding region to regulate cancer cell proliferation.* Proc Natl Acad Sci U S A, 2010. **107**(21): p. 9671-6.
12. Wilkins, S.E., et al., *JMJD5 is a human arginyl C-3 hydroxylase.* Nat Commun, 2018. **9**(1): p. 1180.
13. Fletcher, S.C., et al., *Impaired protein hydroxylase activity causes replication stress and developmental abnormalities in humans.* J Clin Invest, 2023. **133**(7).

14. Gaillard, H., T. Garcia-Muse, and A. Aguilera, *Replication stress and cancer.* Nat Rev Cancer, 2015. **15**(5): p. 276-89.
15. Suzuki, T., et al., *Tumor suppressor gene identification using retroviral insertional mutagenesis in Blm-deficient mice.* EMBO J, 2006. **25**(14): p. 3422-31.
16. Wu, B.H., et al., *Epigenetic silencing of JMJD5 promotes the proliferation of hepatocellular carcinoma cells by down-regulating the transcription of CDKN1A 686.* Oncotarget, 2016. **7**(6): p. 6847-63.
17. Wang, H., et al., *Jumonji-C domain-containing protein 5 suppresses proliferation and aerobic glycolysis in pancreatic cancer cells in a c-Myc-dependent manner.* Cellular Signalling, 2022. **93**: p. 110282.
18. Liu, G., H. Qi, and J. Shen, *JMJD5 inhibits lung cancer progression by regulating glucose metabolism through the p53/TIGAR pathway.* Med Oncol, 2023. **40**(5): p. 145.
19. Chang, W.H., D. Forde, and A.G. Lai, *Dual prognostic role of 2-oxoglutarate-dependent oxygenases in ten cancer types: implications for cell cycle regulation and cell adhesion maintenance.* Cancer Commun (Lond), 2019. **39**(1): p. 23.
20. Marcon, E., et al., *Human-chromatin-related protein interactions identify a demethylase complex required for chromosome segregation.* Cell Rep, 2014. **8**(1): p. 297-310.
21. Wu, J., et al., *RCCD1 depletion attenuates TGF-beta-induced EMT and cell migration by stabilizing cytoskeletal microtubules in NSCLC cells.* Cancer Lett, 2017. **400**: p. 18-29.
22. Cheng, Z., et al., *LINC01419 promotes cell proliferation and metastasis in lung adenocarcinoma via sponging miR-519b-3p to up-regulate RCCD1.* Biochem Biophys Res Commun, 2019. **520**(1): p. 107-114.
23. Hoffman, J.D., et al., *Cis-eQTL-based trans-ethnic meta-analysis reveals novel genes associated with breast cancer risk.* PLoS Genet, 2017. **13**(3): p. e1006690.
24. Islam, M.S., et al., *Structural analysis of the 2-oxoglutarate binding site of the circadian rhythm linked oxygenase JMJD5.* Sci Rep, 2022. **12**(1): p. 20680.
25. Kar, S.P., et al., *Genome-Wide Meta-Analyses of Breast, Ovarian, and Prostate Cancer Association Studies Identify Multiple New Susceptibility Loci Shared by at Least Two Cancer Types.* Cancer Discov, 2016. **6**(9): p. 1052-67.
26. Renault, L., et al., *The 1.7 Å crystal structure of the regulator of chromosome condensation (RCC1) reveals a seven-bladed propeller.* Nature, 1998. **392**(6671): p. 97-101.
27. Petermann, E., et al., *Hydroxyurea-stalled replication forks become progressively inactivated and require two different RAD51-mediated pathways for restart and repair.* Mol Cell, 2010. **37**(4): p. 492-502.
28. Amendola, P.G., et al., *JMJD-5/KDM8 regulates H3K36me2 and is required for late steps of homologous recombination and genome integrity.* PLoS Genet, 2017. **13**(2): p. e1006632.
29. Chakraborty, S., K. Schirmeisen, and S.A. Lambert, *The multifaceted functions of homologous recombination in dealing with replication-associated DNA damages.* DNA Repair (Amst), 2023. **129**: p. 103548.
30. Chun, J., E.S. Buechelmaier, and S.N. Powell, *Rad51 paralog complexes BCDX2 and CX3 act at different stages in the BRCA1-BRCA2-dependent homologous recombination pathway.* Mol Cell Biol, 2013. **33**(2): p. 387-95.
31. Berti, M., et al., *Sequential role of RAD51 paralog complexes in replication fork remodeling and restart.* Nat Commun, 2020. **11**(1): p. 3531.
32. Cai, Q., et al., *Genome-wide association analysis in East Asians identifies breast cancer susceptibility loci at 1q32.1, 5q14.3 and 15q26.1.* Nat Genet, 2014. **46**(8): p. 886-90.
33. Zhong, J., et al., *A Transcriptome-Wide Association Study Identifies Novel Candidate Susceptibility Genes for Pancreatic Cancer.* J Natl Cancer Inst, 2020. **112**(10): p. 1003-1012.

34. Ferreira, M.A., et al., *Genome-wide association and transcriptome studies identify target genes and risk loci for breast cancer.* Nat Commun, 2019. **10**(1): p. 1741.
35. Collins, R.R.J., et al., *Oncometabolites: A New Paradigm for Oncology, Metabolism, and the Clinical Laboratory.* Clin Chem, 2017. **63**(12): p. 1812-1820.
36. Bristow, R.G. and R.P. Hill, *Hypoxia and metabolism. Hypoxia, DNA repair and genetic instability.* Nat Rev Cancer, 2008. **8**(3): p. 180-92.
37. Ray Chaudhuri, A., et al., *Topoisomerase I poisoning results in PARP-mediated replication fork reversal.* Nat Struct Mol Biol, 2012. **19**(4): p. 417-23.
38. Garcin, E.B., et al., *Differential Requirements for the RAD51 Paralogs in Genome Repair and Maintenance in Human Cells.* PLoS Genet, 2019. **15**(10): p. e1008355.
39. Brewitz, L., et al., *5-Substituted Pyridine-2,4-dicarboxylate Derivatives Have Potential for Selective Inhibition of Human Jumonji-C Domain-Containing Protein 5.* J Med Chem, 2023. **66**(15): p. 10849-10865.
40. Hu, C., et al., *Functional and Clinical Characterization of Variants of Uncertain Significance Identifies a Hotspot for Inactivating Missense Variants in RAD51C.* Cancer Res, 2023. **83**(15): p. 2557-2571.
41. Jamal, K., et al., *Drug-gene Interaction Screens Coupled to Tumor Data Analyses Identify the Most Clinically Relevant Cancer Vulnerabilities Driving Sensitivity to PARP Inhibition.* Cancer Res Commun, 2022. **2**(10): p. 1244-1254.
42. Ceccaldi, R., P. Sarangi, and A.D. D'Andrea, *The Fanconi anaemia pathway: new players and new functions.* Nat Rev Mol Cell Biol, 2016. **17**(6): p. 337-49.
43. Hu, S., et al., *Association between XRCC3 rs861539 Polymorphism and the Risk of Ovarian Cancer: Meta-Analysis and Trial Sequential Analysis.* Biomed Res Int, 2022. **2022**: p. 3915402.
44. Tan, S.C., et al., *Association between XRCC3 p.Thr241Met polymorphism and risk of glioma: A systematic review and meta-analysis.* PLoS One, 2022. **17**(10): p. e0276313.
45. Boni, J., et al., *A decade of RAD51C and RAD51D germline variants in cancer.* Hum Mutat, 2022. **43**(3): p. 285-298.
46. Mellacheruvu, D., et al., *The CRAPome: a contaminant repository for affinity purification-mass spectrometry data.* Nat Methods, 2013. **10**(8): p. 730-6.
47. Abramson, J., et al., *Accurate structure prediction of biomolecular interactions with AlphaFold 3.* Nature, 2024. **630**(8016): p. 493-500.
48. Kumar, S., et al., *MEGA X: Molecular Evolutionary Genetics Analysis across Computing Platforms.* Mol Biol Evol, 2018. **35**(6): p. 1547-1549.